




## Article

# A Novel 3D Culture System Using a Chitin-Based Polysaccharide Material Produces High-Quality Allogeneic Human UCMSCs with Dispersed Sphere Morphology

Katsuhiko Kida <sup>1</sup>, Tatsuro Kanaki <sup>1,\*</sup>, Shuang Gao <sup>2</sup>, Daisuke Hatanaka <sup>3</sup>, Masashi Iwakami <sup>1</sup>, Shuai Liu <sup>2</sup>, Masato Horikawa <sup>1</sup>, Minoru Ono <sup>4</sup> and Dehua Chang <sup>5,\*</sup>

- <sup>1</sup> Biological Research Laboratories, Nissan Chemical Corporation, Shiraoka 349-0294, Saitama, Japan; kidak@nissanchem.co.jp (K.K.); iwakamim@nissanchem.co.jp (M.I.); horikawa@nissanchem.co.jp (M.H.)
- <sup>2</sup> BOE Regenerative Medicine Technology Co., Ltd., C2 Building, No.9 Jiuxianqiaobei Road, Chaoyang, Beijing 100015, China; 10143309@boe.com.cn (S.G.); lshuai@boe.com.cn (S.L.)
- <sup>3</sup> Materials Research Laboratories, Nissan Chemical Corporation, Funabashi 274-0052, Chiba, Japan; hatanakad@nissanchem.co.jp
- <sup>4</sup> Department of Cardiac Surgery, University of Tokyo Hospital, 7-3-1 Hongo, Bunkyo-ku 113-8655, Tokyo, Japan; ono-tho@h.u-tokyo.ac.jp
- <sup>5</sup> Department of Cell Therapy in Regenerative Medicine, University of Tokyo Hospital, 7-3-1 Hongo, Bunkyo-ku 113-8655, Tokyo, Japan
- \* Correspondence: kanaki@nissanchem.co.jp (T.K.); jot.sur@mail.u-tokyo.ac.jp (D.C.); Tel.: +81-480-92-2513 (T.K.); +81-3-3815-5411 (D.C.)



**Citation:** Kida, K.; Kanaki, T.; Gao, S.; Hatanaka, D.; Iwakami, M.; Liu, S.; Horikawa, M.; Ono, M.; Chang, D. A Novel 3D Culture System Using a Chitin-Based Polysaccharide Material Produces High-Quality Allogeneic Human UCMSCs with Dispersed Sphere Morphology. *Cells* **2022**, *11*, 995. <https://doi.org/10.3390/cells11060995>

Academic Editor: Joni H. Ylostalo

Received: 9 February 2022

Accepted: 13 March 2022

Published: 15 March 2022

**Publisher's Note:** MDPI stays neutral with regard to jurisdictional claims in published maps and institutional affiliations.



**Copyright:** © 2022 by the authors. Licensee MDPI, Basel, Switzerland. This article is an open access article distributed under the terms and conditions of the Creative Commons Attribution (CC BY) license (<https://creativecommons.org/licenses/by/4.0/>).

**Abstract:** Mesenchymal stem cell (MSC) transplantation, in particular allogeneic transplantation, is a promising therapy for a variety of diseases. However, before performing allograft treatment it is necessary to find suitable donors, establish culture methods that maintain cell quality, and reduce cell production costs. Here, we present a new method of producing allogeneic MSCs combining human umbilical cord-derived mesenchymal stem cells (UCMSCs) and chitin-based polysaccharide fibers (Cellhesion<sup>®</sup> MS). UCMSC numbers significantly increased, and cells grew as dispersed spheres on Cellhesion<sup>®</sup> MS. Subsequent biological analyses showed that the expression levels of stemness-related and migration-related genes were significantly upregulated, including octamer-binding transcription factor 4 (OCT4), Nanog homeobox (NANOG), and C-X-C chemokine receptor type 4 (CXCR4). The secretion levels of paracrine factors such as prostaglandin E2 (PGE<sub>2</sub>), TNF $\alpha$ -stimulating gene (TSG)-6, fibroblast growth factor 2 (bFGF), and Angiogenin (Ang) from UCMSCs using Cellhesion<sup>®</sup> MS were significantly higher than with microcarrier and U-bottom plate culture. In addition, culture supernatant from UCMSCs with Cellhesion<sup>®</sup> MS had better angiogenic potential than that from monolayer cultured UCMSCs. Furthermore, we succeeded in a scaled-up culture of UCMSCs with Cellhesion<sup>®</sup> MS using a closed culture bag. Therefore, Cellhesion<sup>®</sup> MS is a key material for producing high-quality UCMSCs in a three-dimensional (3D) culture system.

**Keywords:** human umbilical cord mesenchymal stem cells; 3D culture; allogeneic transplantation; paracrine factors; stemness

## 1. Introduction

Mesenchymal stem cells (MSCs) isolated from various organs and tissues, such as bone marrow, adipose tissues, and umbilical cords, can be differentiated into adipocytes, chondrocytes, osteoblasts, cartilage, bone, skeletal muscle, and other cell types in specific conditions [1–4]. MSCs are applicable as treatment in a wide range of diseases (e.g., heart, immune, and inflammatory diseases), as based on their effects in immunomodulation, anti-inflammation, and angiogenesis. As a result clinical trials are underway [5,6]. MSCs secrete various paracrine factors, such as immunosuppressive factors, angiogenic factors, anti-apoptotic factors, and anti-oxidative factors involved in repair of damage of the

endometrium and inhibition of the graft versus host response function [5]. Additionally, recent reports indicate that extracellular vesicles (EVs) present in MSC culture supernatants have a therapeutic effect on disease states [7,8]. Thus, MSC culture systems are capable of simultaneously producing two sources of therapeutics: the cells themselves, and culture supernatants containing EVs.

The two most common settings for stem cell transplantation are autologous and allogeneic. Although autologous MSC transplantation is the safest method, as there is no immune rejection, it may have some limitations in terms of time, cost, and quality [9]. Allogeneic MSC transplantation has attracted attention recently. One report suggested that the immunosuppressive properties and low immunogenicity of allogeneic MSCs effect a reduced immune response after transplantation [9]. Thus, allogeneic MSC transplantation have more potential and prospect in clinical application. It has also been reported that UCMSCs show higher OCT4 expression and have higher immunosuppressive effects than bone marrow-derived MSCs (BMMSCs) [10]. Therefore, UCMSCs are considered as a promising cell source for cell therapy.

For allogeneic MSC production, monolayer culture is the most conventional culture method. However, the spindle shape of cells observed in monolayer culture is not observed *in vivo*. When MSCs are cultured in monolayer conditions, the cell diameter increases with each passage, while the growth rate, stemness gene expression, and secretion of paracrine factors decrease [11–13]. Although a method for scaled-up MSC culture using microcarriers has been described, MSCs attached to carrier beads exhibit the same spindle shape observed in monolayer culture. In contrast, a suspension culture in stirring conditions which uses an ultra-low attachment plate and other 3D materials has produced MSCs with a round morphology [11]. However, MSCs undergo cell cycle arrest when cultured in these conditions, and cells cultured for extended periods undergo apoptosis-like anoikis due to the lack of scaffolding, which ultimately results in cell death [14]. To produce MSCs in 3D cell culture, it is essential not only to maintain quality but also to expand the MSCs.

Recently, we reported a 3D culture of UCMSCs using a chitin-based polysaccharide material [15]. This material enables EVs to be collected more efficiently, and EVs secreted from 3D cultured MSCs have higher immune-modulating potential than those from monolayer culture. However, pipetting was needed to culture MSCs with Cellhesion<sup>®</sup> VP because of severe aggregation. Cellhesion<sup>®</sup> MS is an insoluble chitin-based polysaccharide fiber. One unique characteristic of Cellhesion<sup>®</sup> MS is that cells adhere to and proliferate on this material with a round shape, as *in vivo*. In addition, this material plays a role as a dispersant of MSC spheres. Therefore, aggregation is suppressed compared with Cellhesion<sup>®</sup> VP.

In this study we evaluated the effect of a 3D culture using Cellhesion<sup>®</sup> MS on the characteristics of UCMSCs. Significant up-regulation was observed in gene expression (OCT4, NANOG, and CXCR4) and paracrine factors (PGE<sub>2</sub>, TSG-6, bFGF, and Ang). In addition, Cellhesion<sup>®</sup> MS enables the culture of UCMSCs with the suppression of large cell aggregation in large-scale conditions. Thus, this new 3D culture method is suitable for producing high-quality UCMSCs at large scale that are highly suitable for allogeneic stem cell transplantation.

## 2. Materials and Methods

### 2.1. Chemicals and Reagents

Cellhesion<sup>®</sup> MS was obtained from Nissan Chemical Corporation. Human UCMSCs, Mesenchymal Stem Cell Growth Medium 2, human umbilical vein endothelial cells (HUVEC), Endothelial Cell Growth Medium, Endothelial Cell Basal Medium, DetachKit, PrimeScript<sup>™</sup> RT Master Mix (Perfect Real Time), and Premix Ex Taq<sup>™</sup> (Perfect Real Time) were purchased from Takara (Kusatsu, Shiga, Japan). MEM $\alpha$  with L-glutamine and Phenol Red was obtained from Fujifilm Wako Pure Chemical Corporation (Osaka, Osaka, Japan). The RNeasy mini kit was purchased from Qiagen (Valencia, CA, USA). All Taqman probes, Nunc MaxiSorp<sup>™</sup> flat-bottom plates, FBS, nonessential amino acids, and BrdU staining kits

were obtained from Thermo Fisher Scientific (Waltham, MA, USA). Recombinant human TNF $\alpha$ , human TSG-6 biotinylated antibody, and recombinant human TSG-6 were obtained from R&D Systems (Minneapolis, MN, USA). TSG-6 antibody was obtained from Santa Cruz Biotechnology (Dallas, TX, USA). Streptavidin (HRP) was purchased from Abcam (Trumpington, Cambridge, UK). TMB 1-Component Microwell Peroxidase Substrate, Sure-Blue, and TMB Stop Solution were obtained from SeraCare Life Sciences (Milford, MA, USA). The PGE<sub>2</sub> ELISA kit was obtained from Enzo Life Sciences (Farmingdale, NY, USA). The bFGF ELISA kit was obtained from RayBiotech (Peachtree Corners, GA, USA). The Angiogenin ELISA kit was purchased from Proteintech (Rosemont, IL, USA). Culture bags were purchased from Nipro (Osaka, Osaka, Japan). Corning<sup>®</sup> Matrigel<sup>®</sup> Growth Factor Reduced (GFR) Basement Membrane Matrix, Phenol Red-free, LDEV-free, Costar<sup>®</sup> 6-well and 24-well clear flat-bottomed ultra-low attachment well plates, Costar<sup>®</sup> 24-well clear TC-treated well plates,  $\alpha$ -MEM medium, RPMI 1640 medium, L-glutamine, 125 mL disposable spinner flasks, and Corning<sup>®</sup> low-concentration Synthemax<sup>™</sup> II microcarriers were obtained from Corning Incorporated (Corning, NY, USA). The CellTiter-Glo<sup>®</sup> Luminescent Cell Viability Assay was obtained from Promega (Madison, WI, USA). Cell Counting Kit-8 and Cellstain<sup>®</sup> (Calcein-AM) were obtained from Dojindo Laboratories (Kumamoto, Kumamoto, Japan). Anti-CD11b-PE (clone no. ICRF44), anti-CD19-FITC (clone no. HIB19), anti-CD34-PE (clone no. 581), anti-CD45-APC-cy7 (clone no. 2D1), anti-CD73-PE (clone no. AD2), anti-CD90-FITC (clone no. 5E10), anti-CD105-APC (clone no. 266), anti-HLA-DR-APC (clone no. G46-6), and stain buffer were obtained from BD Biosciences (Franklin Lakes, NJ, USA). Adipogenic, chondrogenic, and osteogenic differentiation kits were purchased from Cyagen (Santa Clara, CA, USA). Cell cycle kits were obtained from KeyGEN BioTECH (Nanjing, Jiangsu, China). PHA-L and Interleukin (IL)-2 were obtained from Sigma (Saint Louis, MO, USA). All other chemicals and solvents were of the highest grades that were commercially available.

### 2.2. Isolation of Umbilical Cord Mesenchymal Stromal Cells

Umbilical cord samples were collected from donors during childbirth. The criteria for selection of umbilical cord tissues were that they were from a full-term birth and were negative for HIV, HBV, HCV, HCMV, EBV, HTLV, HPV, and human parvovirus B19.

The umbilical cord samples were cut into 3 cm lengths and veins, arteries, and the tunica externa were removed. Next, the sample was washed three times with PBS, and cut into 1–2 mm<sup>3</sup> fragments. The fragments were then uniformly placed in 100 mm diameter culture dishes with approximately 5 mm spacing. Finally, 4 mL of culture medium ( $\alpha$ -MEM medium with 10% FBS, 1% nonessential amino acid, 1% L-glutamine, 4 ng/mL bFGF, and 40 unit/mL gentamicin) was added to each culture dish. The culture dishes were placed in an incubator at 37 °C, with 5% CO<sub>2</sub> and 95% humidity. The culture medium was completely replaced every three days until cells migrated from the fragments and reached 70% confluence. The tissues were then removed, and the cells were passaged at a ratio of 1:4. Cells from the fourth passage were used in subsequent experiments.

### 2.3. Identity and Purity

UCMSC morphology was observed under an inverted microscope (Olympus CKX41; Shinjuku-ku, Tokyo, Japan) and images were captured with a camera (Canon EOS 700D; Ota-ku, Tokyo, Japan). Cellular phenotypes were evaluated for CD11b, CD19, CD34, CD45, CD73, CD90, CD105, and HLA-DR expression. The UCMSCs were washed twice in stain buffer prior to staining with anti-CD11b-PE, anti-CD19-FITC, anti-CD34-PE, anti-CD45-APC-cy7, anti-CD73-PE, anti-CD90-FITC, anti-CD105-APC, anti-HLA-DR-APC and isotype control antibodies for 30 min at room temperature and in the dark. The UCMSCs were then washed twice in stain buffer and re-suspended in 0.5 mL of stain buffer for flow cytometry. UCMSCs stained with isotype-APC, isotype-APC-cy7, isotype-FITC, and isotype-PE were used as respective controls.

UCMSCs can differentiate toward adipogenic cells, chondroblasts, and osteoblasts. Thus, adipogenic, chondrogenic, and osteogenic differentiation kits were used in accordance with the supplier's specifications. Finally, adipogenic, chondrogenic, and osteogenic differentiation was evaluated by oil red O staining, alcian blue staining, and alizarin red staining, respectively.

#### 2.4. Cell Cycle Analysis

The cell cycle was analyzed using a cell cycle kit. Briefly,  $1 \times 10^6$  UCMSCs were fixed in 1 mL of 70% ice-cold ethanol overnight. The fixed cells were then washed twice with PBS. Next, 100  $\mu$ L of RNase A was added and the cells were incubated at 37 °C for 30 min. After washing once with PBS, the fixed cells were suspended in 400  $\mu$ L of PI staining solution for 30 min at 4 °C in the dark. Finally, the cell suspension was evaluated by flow cytometry.

#### 2.5. Immunosuppressive Function

The immunosuppressive function of UCMSCs was evaluated by inhibiting peripheral blood mononuclear cells (PBMCs) proliferation, and a BrdU staining kit was used to label PBMCs and assess proliferation. UCMSCs were seeded into 6-well plates at a density of  $5 \times 10^4$  cells/cm<sup>2</sup>. When the UCMSC confluence reached 70%, PBMCs were seeded in the wells containing UCMSCs at a density of  $1.25 \times 10^5$  cells/cm<sup>2</sup>. 3 mL of RPMI 1640 medium containing 10% (*v/v*) FBS, 10  $\mu$ g/mL of PHA-L, and 10 ng/mL of IL-2 was added to each well to activate PBMCs. The culture medium was changed two days later. On the fourth day, BrdU was added to the culture medium at a concentration of 10  $\mu$ M. Cultivation of activated PBMCs alone was used as the positive control. Nonactivated PBMCs co-cultured with UCMSCs was used as the negative control. After 16 h, the PBMCs were collected and stained in accordance with the supplier's instructions and evaluated by flow cytometry.

#### 2.6. Human UCMSC Culture with Cellhesion<sup>®</sup> MS

For monolayer culture, UCMSCs were cultured at passages 3 to 5. UCMSCs were seeded at a density of 15,000 cells/mL into Mesenchymal Stem Cell Growth Medium 2 containing 0.05% (*w/v*) of Cellhesion<sup>®</sup> MS and dispensed into clear flat-bottomed ultra-low attachment 6-well plates or a culture bag (10 mL/well or 45 mL/culture bag). Half of the culture supernatant was removed and replaced with fresh medium every 3–4 days. The plates and culture bag were cultured unstirred for 1–2 weeks. Viable cells were counted by measurement of absorbance at 450 nm, using a SpectraMax<sup>®</sup> 190 (Molecular Devices; San Jose, CA, USA) for the CCK-8 assay. For the ATP assay, an equal volume of ATP reagent (CellTiter-Glo<sup>®</sup> Luminescent Cell Viability Assay) was added to the culture medium and the luminescent intensity (relative light unit (RLU) value) was measured using Enspire<sup>™</sup> (PerkinElmer; Waltham, MA, USA) at each time point. Cultured UCMSCs were stained by Cellstain<sup>®</sup> at each time point.

#### 2.7. Human UCMSC Culture with Microcarrier and in U Bottom Plates

UCMSCs were seeded at a density of 15,000 cells/mL into 45 mL of Mesenchymal Stem Cell Growth Medium 2 containing 400 mg of Corning<sup>®</sup> low-concentration Synthe-max<sup>™</sup> II microcarriers and dispensed into a 125 mL spinner flask. For U-bottom plate culture, UCMSCs were seeded at a density of 15,000 cells/mL (200  $\mu$ L/well). When using microcarriers, cell adhesion occurred in static conditions for 24 h after which cultures were agitated at 30 rpm for 15 min every three hours. Half of the culture supernatant was removed and replaced with fresh medium after four days.

#### 2.8. Scanning Electron Microscopy (SEM) Evaluation

Sample preparation for scanning electron microscopy (SEM) was as follows. UCMSCs cultured with Cellhesion<sup>®</sup> MS were fixed in 2% glutaraldehyde for three hours. The fixed UCMSCs and Cellhesion<sup>®</sup> MS were then washed with PBS and immersed in ethanol for

two hours, for dehydration. The resulting specimen was then washed with tert-butyl alcohol and applied to a glass plate. The specimen was then lyophilized, and Pt sputtering deposition was performed. SEM images were obtained using a Hitachi SU-8000 electron microscope (Hitachi, Ltd; Chiyoda-ku, Tokyo, Japan). The accelerated voltage of the electron beam was 1.7 kV.

### 2.9. RNA Isolation and Real-Time PCR

Total RNA was prepared using a RNeasy mini kit in accordance with the manufacturer's protocols. The cDNA was synthesized from total RNA using PrimeScript™ RT Master Mix (Perfect Real Time). Real-time RT-PCR was performed using Premix Ex Taq™ (Perfect Real Time) with a 7500/7500 Fast Real-Time PCR System (Applied Biosystems; Waltham, MA, USA). The Taqman probes for NANOG, OCT4, C-X-C chemokine receptor type 4 (CXCR4), and glyceraldehyde-3-phosphate dehydrogenase (GAPDH) were Hs04399610\_g1, Hs04260367\_gH, Hs00607978\_s1, and Hs99999905\_m1, respectively. The PCR conditions for these genes were as follows: after an initial denaturation at 95 °C for 10 s, amplification was performed by denaturation at 95 °C for 10 s and annealing and extension at 60 °C for 34 s and 45 cycles. NANOG, OCT4, and CXCR4 mRNA levels were normalized to GAPDH mRNA.

### 2.10. Enzyme-Linked Immunosorbent Assay (ELISA) of PGE<sub>2</sub>, TSG-6, bFGF, and Angiogenin in Culture Supernatants

UCMSCs were seeded at a density of 50,000 cells/mL in Mesenchymal Stem Cell Growth Medium 2 containing 0.05% (*w/v*) of Cellhesion® MS and dispensed into a clear flat-bottomed ultra-low attachment 24-well plate at 1 mL/well. For monolayer culture, UCMSCs were seeded at a density of 50,000 cells/mL in Mesenchymal Stem Cell Growth Medium 2 without Cellhesion® MS and dispensed into a Costar® clear TC-treated 24-well plate at 1 mL/well. These plates were cultured unstirred for 48 h, after which the cells were switched to fresh Mesenchymal Stem Cell Growth Medium 2 with or without 20 ng/mL recombinant human TNF $\alpha$  or MEM $\alpha$  with L-glutamine and phenol red containing 17% FBS, which is based on the previously reported conditions [16]. TNF $\alpha$  was treated to imitate the situation when inflammation was triggered. Cells were cultured for a further 24 h, after which the culture supernatants were harvested and viable cells were counted by measurement of absorbance or ATP assay, as described above. The quantification of PGE<sub>2</sub>, bFGF, and Angiogenin in culture supernatants was performed in accordance with the manufacturer's protocols. The quantification of TSG-6 in culture supernatants was performed by ELISA and according to the conventional procedure, as follows: a Nunc MaxiSorp™ flat-bottomed ELISA plate was coated with a rat monoclonal antibody against hTSG-6. Human TSG-6 biotinylated antibody and streptavidin (HRP) were used for the primary and secondary detection antibodies, respectively. TMB 1-Component Microwell Peroxidase Substrate, SureBlue, and TMB Stop Solution were used for detection, and absorbance at 450 nm was measured using Enspire™. TSG-6 concentrations were determined with a standard curve constructed by titrating rhTSG-6 (0–50 ng/mL).

### 2.11. Tube Formation Assay

For monolayer culture, HUVEC were cultured at passages 2–3. After the Matrigel® was thawed, a pre-cooled 96 well plate was loaded with the Matrigel® at 100  $\mu$ L/well and placed in the culture incubator for 1 h. Then, HUVEC at a density of 2000 cells/50  $\mu$ L Endothelial Cell Basal Medium/well were seeded in the 96 well plate and incubated with 50  $\mu$ L conditioned medium harvested as above. After 4 h, the tubes were imaged using an inverted light microscope and quantified by the Angiogenesis Analyzer plug-in on ImageJ software.

### 2.12. Statistical Analyses

Statistical significance was analyzed with a Student's *t*-test or Tukey's test as indicated in each legend, using EXSAS version 7.1.6.1 (Arm System; Osaka, Osaka, Japan). The level of significance was set at 0.05 unless stated otherwise.

## 3. Results

### 3.1. Features of Cellhesion<sup>®</sup> MS Culture

To investigate the basic characteristics of Cellhesion<sup>®</sup> MS culture, we analyzed the morphology of UCMSCs with Cellhesion<sup>®</sup> MS using a microscope. When UCMSCs prepared in monolayer culture were seeded with Cellhesion<sup>®</sup> MS, almost all cells adhered to Cellhesion<sup>®</sup> MS within 24 h. When Cellhesion<sup>®</sup> MS was in the medium under static conditions, it accumulated and formed weak aggregates; however, the weak aggregates were reversibly dispersed and induced to float with gentle stirring. We observed increased MSC cell–cell adhesion, proliferation, and formation of dispersed spheres with Cellhesion<sup>®</sup> MS, which suppressed the formation of large cell aggregates in 3D culture condition. The size of spheres was around 300  $\mu\text{m}$  (Figure 1A). A schematic representation of Cellhesion<sup>®</sup> MS culture is also shown in Figure 1A. In addition, we analyzed Cellhesion<sup>®</sup> MS and the morphology of UCMSCs with Cellhesion<sup>®</sup> MS by SEM. Cellhesion<sup>®</sup> MS exhibited a fiber-like structure in the medium (Figure 1B). Interestingly, the morphology of the attached MSCs remained round (Figure 1B). To confirm the number of UCMSCs increase, we evaluated the cell growth by ATP assay. The number of UCMSCs increased significantly by 5.8 times and 12.6 times at four and seven days ( $p < 0.05$  and  $p < 0.01$ , respectively) (Figure 1C). Furthermore, to verify the effect of 3D culture using Cellhesion<sup>®</sup> MS, we evaluated the expression levels of stemness-related genes such as OCT4 and NANOG and the migration-related gene, CXCR4. OCT4, NANOG, and CXCR4 mRNA expression levels in UCMSCs cultured with Cellhesion<sup>®</sup> MS were significantly higher than UCMSCs at day zero ( $p < 0.001$ ,  $p < 0.01$ , and  $p < 0.05$ , respectively) (Figure 1D). This result indicates that stemness- and migration-related genes in UCMSCs were upregulated in Cellhesion<sup>®</sup> MS culture. Thus, UCMSCs could attach to and grow on Cellhesion<sup>®</sup> MS, and the morphology of UCMSCs with Cellhesion<sup>®</sup> MS differed from monolayer cultured MSCs. In addition, MSCs cultured with Cellhesion<sup>®</sup> MS were able to gain enhanced stemness and migration ability.

### 3.2. Paracrine Factors from UCMSCs with Cellhesion<sup>®</sup> MS

MSCs have immunomodulation, anti-inflammation, and angiogenesis effects resulting from secretion of paracrine factors. To verify the effects of 3D culture using Cellhesion<sup>®</sup> MS, we evaluated typical paracrine factors from UCMSCs in each category compared with monolayer culture. We found that the secretion levels of PGE<sub>2</sub> (immunomodulation) and TSG-6 (anti-inflammation) from UCMSCs with Cellhesion<sup>®</sup> MS were significantly higher than from monolayer culture, whether with or without TNF $\alpha$  treatment ( $p < 0.001$  and  $p < 0.01$ , respectively) (Figure 2A). Treatment with TNF $\alpha$  of UCMSCs with Cellhesion<sup>®</sup> MS resulted in a significant induction of PGE<sub>2</sub> and TSG-6 secretion (by 2.2 times and 1.6 times, respectively) ( $p < 0.001$  and  $p < 0.01$ , respectively). In addition, the secretion levels of bFGF and Angiogenin (angiogenesis) from UCMSCs with Cellhesion<sup>®</sup> MS were significantly higher than levels from cells in monolayer culture ( $p < 0.01$  and  $p < 0.05$ , respectively) (Figure 2B). To evaluate the function of UCMSCs, the tube formation assay was performed using conditioned medium (CM) from each culture condition. The total length of HUVEC treated with CM from UCMSCs with Cellhesion<sup>®</sup> MS was significantly longer than the control and CM from monolayer cultured UCMSCs ( $p < 0.001$ ) (Figure 2C). Thus, MSCs cultured with Cellhesion<sup>®</sup> MS were able to secrete far more paracrine factors, properties likely to affect treatment efficacy.

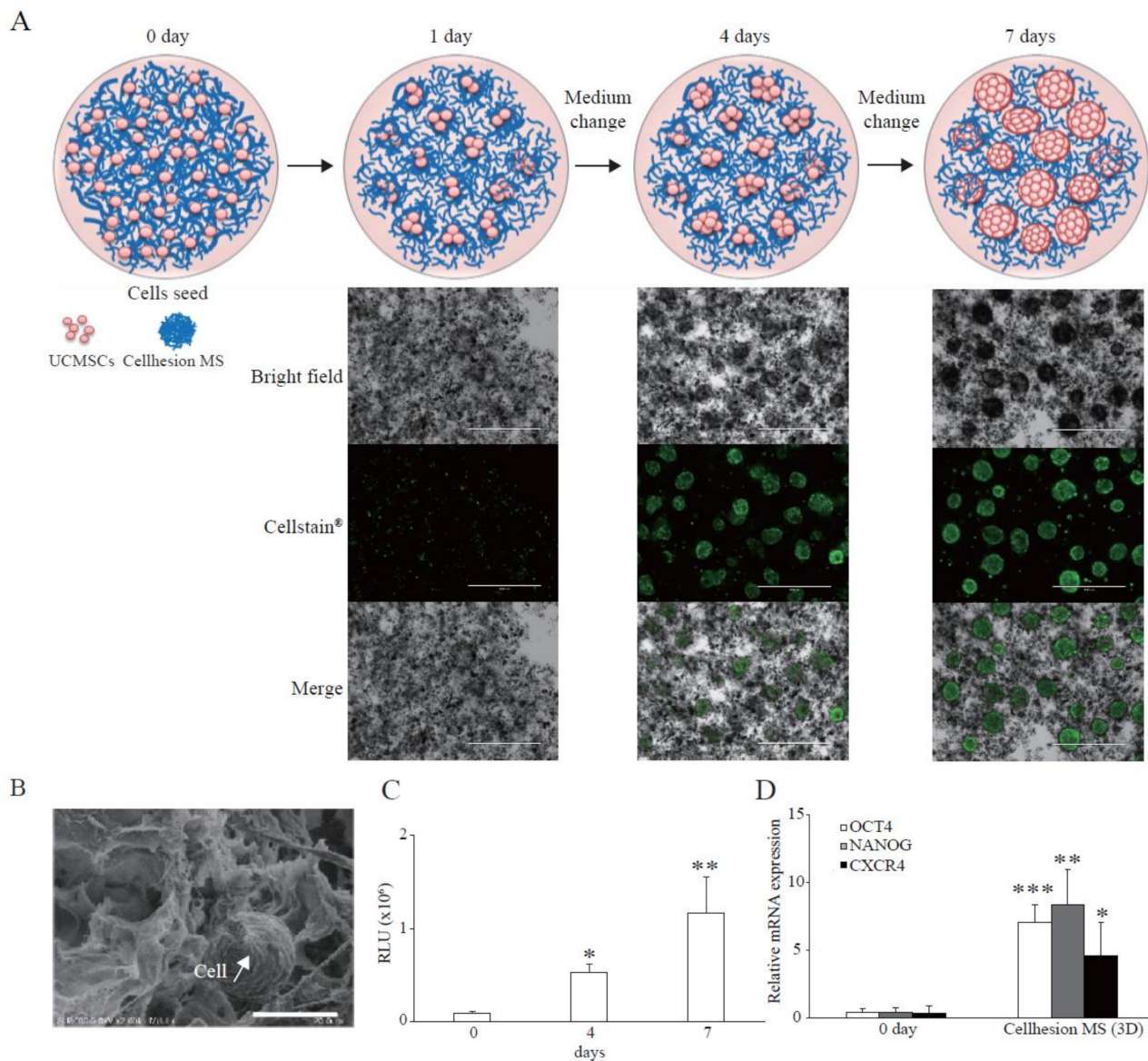


**Figure 1.** Features of Cellhesion® MS culture. **(A)** Images of Cellhesion® MS culture. Schematic representation of Cellhesion® MS culture. Blue lines indicate Cellhesion® MS and pink spheres indicate MSCs. UCMSCs were stained green by Cellstain®. Scale bar = 1000  $\mu$ m. **(B)** SEM images of Cellhesion® MS and UCMSCs. White arrows indicate UCMSCs. Scale bar = 20  $\mu$ m. **(C)** The number of UCMSCs increased in a time-dependent manner. The number of UCMSCs was measured using an ATP assay. \*  $p < 0.05$ , \*\*  $p < 0.01$ , compared with day zero. **(D)** The expression levels of NANOG, OCT4, and CXCR4 mRNA in UCMSCs increased. The expression levels of NANOG, OCT4, and CXCR4 mRNA in UCMSCs were determined by real-time RT-PCR and normalized to GAPDH mRNA levels. \*  $p < 0.05$ , \*\*  $p < 0.01$ , \*\*\*  $p < 0.001$  compared with day zero. Data show mean averages  $\pm$  SD for three independent experiments.

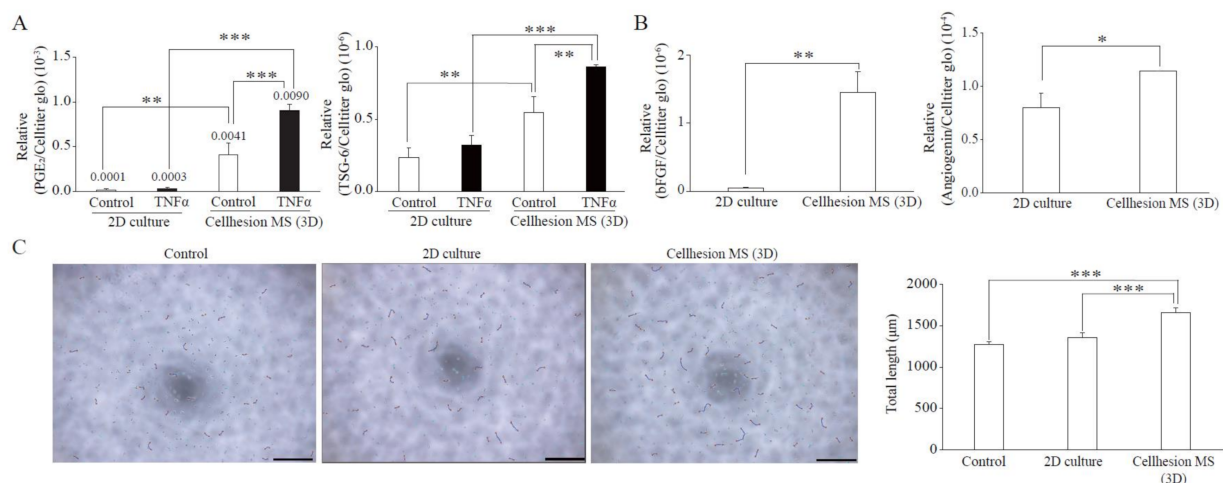


**Figure 2.** Paracrine factors from UCMSCs with Cellhesion<sup>®</sup> MS. **(A)** The secretion levels of PGE<sub>2</sub> and TSG-6 by UCMSCs cultured with Cellhesion<sup>®</sup> MS increased, compared with monolayer culture. The secretion levels of PGE<sub>2</sub> and TSG-6 by UCMSCs were measured by ELISA and normalized with an ATP assay. \*\*  $p < 0.01$ , \*\*\*  $p < 0.001$ , compared with each control or TNF $\alpha$ . **(B)** The secretion levels of bFGF and Angiogenin by UCMSCs cultured with Cellhesion<sup>®</sup> MS increased, compared with monolayer culture. The secretion levels of bFGF, and Angiogenin by UCMSCs were measured by ELISA and normalized with an ATP assay. \*  $p < 0.05$ , \*\*  $p < 0.01$ , compared with each culture. **(C)** The total length of HUVEC treated with CM from UCMSCs with Cellhesion<sup>®</sup> MS was significantly longer than control and with CM from monolayer cultured UCMSCs. Total length of HUVEC in each condition was calculated by Angiogenesis Analyzer plug-in on ImageJ software. Each picture was one of the analyzed examples. Scale bar = 500  $\mu\text{m}$ . \*\*\*  $p < 0.001$ , compared with control or CM from monolayer cultured UCMSCs. Data show mean averages  $\pm$  SD for three independent experiments.

### 3.3. Characterization of UCMSCs from Donors

We established primary UCMSCs to apply Cellhesion<sup>®</sup> MS culture. The umbilical cord samples used in this study were provided by donors at the time of childbirth. Initially, we investigated the basic characteristics of these established UCMSCs. Primary UCMSCs were usually observed 10–14 days after seeding tissue fragments. UCMSCs adhered well to the culture dish surface. P1 and P4 UCMSCs exhibited a fibroblast-like shape (Figure 3A). P10 UCMSCs exhibited a flat and elongated shape (Figure 3A). UCMSCs were positive for the common MSC markers: CD73 (96.3%), CD90 (99.4%), and CD105 (98%) (Figure 3B). UCMSCs were negative (or low) for the hematopoietic markers CD11b (0.024%), CD19 (0.042%), CD34 (0.011%), CD45 (1.14%), and HLA-DR (0.012%) (Figure 3B). UCMSCs were successfully differentiated into osteoblasts, adipocytes, and chondroblasts after 21 days of induction. The differentiated samples stained positive with alizarin red, oil red O, and alcian blue, respectively (Figure 3C). A cell cycle analysis indicated that 45.6% of UCMSCs were in the G<sub>0</sub>/G<sub>1</sub> phase, 42.1% in the S phase, and 12.3% in the G<sub>2</sub>/M phase (Figure 3D). Immunosuppression studies indicated that UCMSCs effectively inhibited the proliferation of PBMCs. Results showed that the percent of new growing PBMCs reduced, from 4.39% to 1.46% during 16 h, when co-cultured with UCMSCs (Figure 3E).



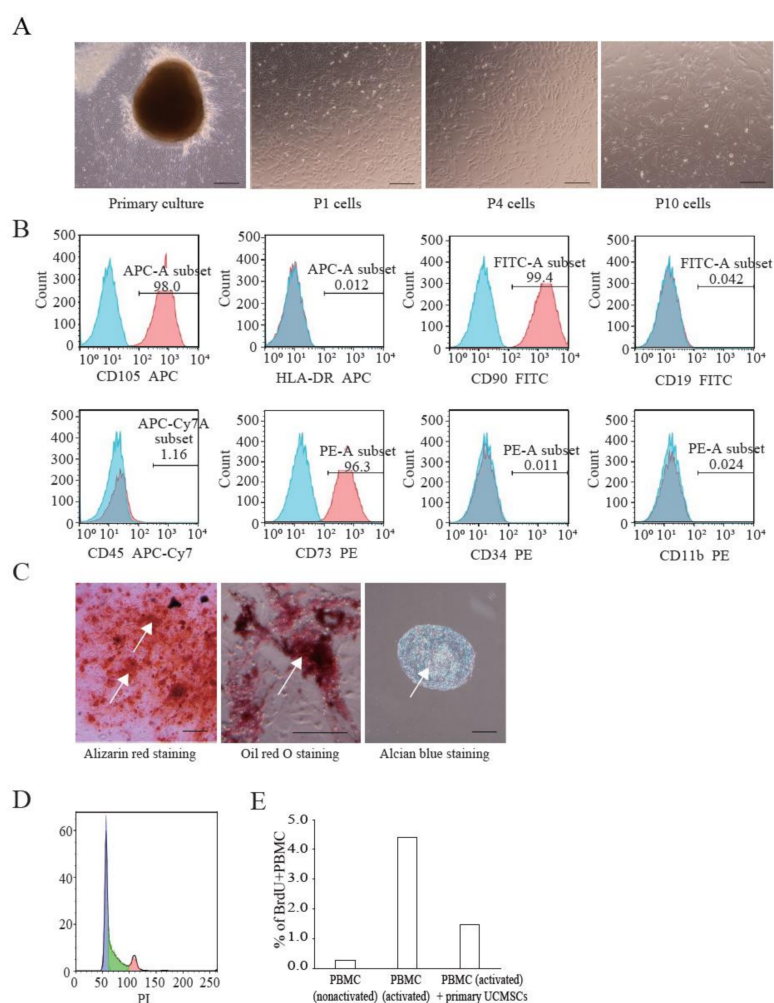


**Figure 3.** Characterization of UCMSCs from donors. **(A)** Culture and expansion of UCMSCs. Scale bar = 250  $\mu$ m. **(B)** Representative flow cytometry histograms of human UCMSCs. UCMSCs were positive for CD105, CD90, and CD73, and negative for CD11b, CD19, CD34, CD45, and HLA-DR. Blue histograms are isotype controls and red histograms are experimental samples. **(C)** UCMSCs were successfully differentiated into adipogenic cells, chondroblasts, and osteoblasts. White arrows indicate stained cells. Scale bar = 500  $\mu$ m. **(D)** Cell cycle analysis. **(E)** UCMSCs inhibit PBMC proliferation.

### 3.4. Confirmation of Characteristics of Cellhesion<sup>®</sup> MS Culture Using UCMSCs from Donors

To investigate differences between the four donors in terms of the effects of Cellhesion<sup>®</sup> MS, and the difference between commercial UCMSCs and UCMSCs, we examined 3D cultures of four UCMSCs established from donor samples. In this culture, all primary UCMSCs formed spheres on Cellhesion<sup>®</sup> MS (Figure 4A). Firstly, we evaluated the cell growth of UCMSCs; the number of UCMSCs significantly increased at eight days ( $p < 0.01$ ) (Figure 4B). Next, we evaluated the expression levels of stemness-related genes and demonstrated that OCT4 and NANOG mRNA were upregulated, compared to day zero and a monolayer culture (Figure 4C). Finally, we evaluated paracrine factors from UCMSCs. The secretion level of PGE<sub>2</sub> from primary UCMSCs with Cellhesion<sup>®</sup> MS was significantly higher than monolayer cultured primary UCMSCs with TNF $\alpha$  ( $p < 0.001$ ) and without TNF $\alpha$  ( $p < 0.01$ ) (Figure 4D). The treatment of UCMSCs on Cellhesion<sup>®</sup> MS with TNF $\alpha$  resulted in a significant ( $p < 0.01$ ) induction of PGE<sub>2</sub> secretion (by 1.9 times). The secretion levels of bFGF from UCMSCs with Cellhesion<sup>®</sup> MS was significantly higher than monolayer cultured UCMSCs ( $p < 0.001$ ) (Figure 4D). Thus, we obtained almost the same results for

cell growth, gene expression, and paracrine factors with commercial and UCMSCs. These results suggest that this culture system could be suitable for any type of UCMSCs.

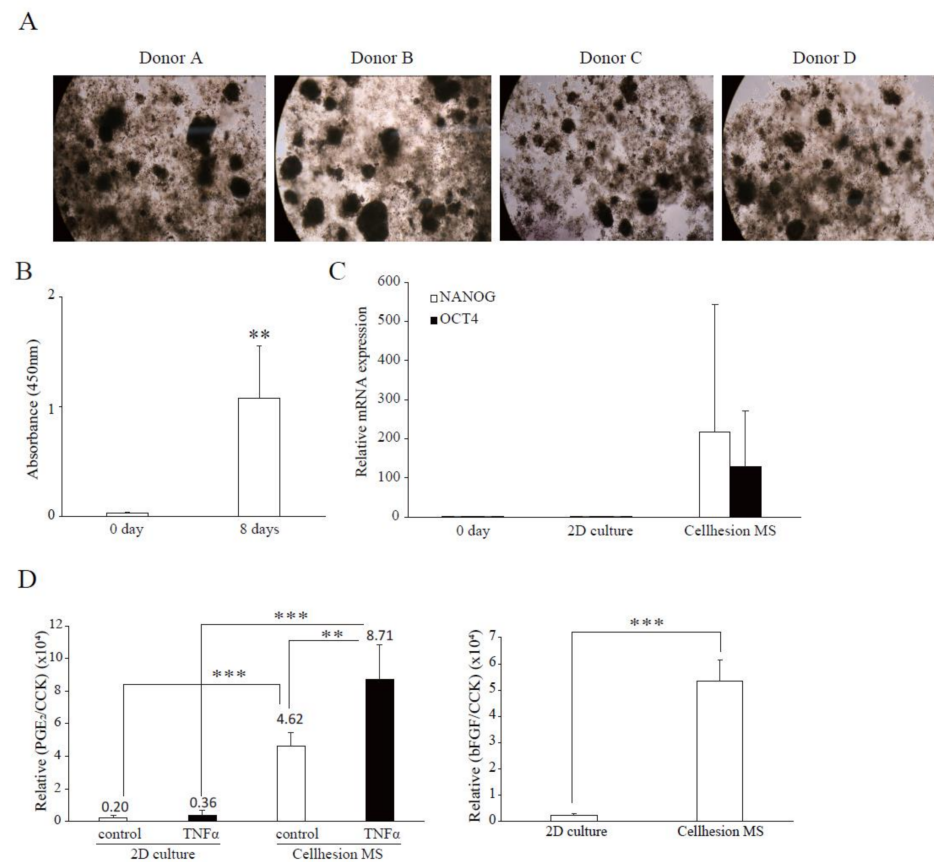


**Figure 4.** Confirmation of characteristics of Cellhesion<sup>®</sup> MS culture, using UCMSCs from donors. (A) Images of cell morphology for each donor. (B) The number of primary UCMSCs from donors increased. The number of primary UCMSCs was measured using an ATP assay. \*\*  $p < 0.01$ , compared with day zero. (C) The expression levels of NANOG and OCT4 mRNA in UCMSCs on Cellhesion<sup>®</sup> MS increased, compared with day zero and monolayer culture. The expression levels of NANOG and OCT4 mRNA in UCMSCs were determined by real-time RT-PCR and normalized to GAPDH mRNA levels. (D) The secretion levels of PGE<sub>2</sub> and bFGF from UCMSCs cultured with Cellhesion<sup>®</sup> MS increased, compared with monolayer culture. The secretion levels of PGE<sub>2</sub> and bFGF from UCMSCs were measured by ELISA and normalized with a CCK assay. \*\*  $p < 0.01$ , \*\*\*  $p < 0.001$ , compared with control or TNF $\alpha$ . Data show mean averages  $\pm$  SD for four independent donors.

### 3.5. Scaled-Up Culture of UCMSCs Using a Culture Bag in a Closed Culture System

To evaluate the possibility of large-scale UCMSC culture using Cellhesion<sup>®</sup> MS, and for comparison with other culture methods, we attempted to culture UCMSCs with Cellhesion<sup>®</sup> MS in a culture bag format (Figure 5A). Firstly, we evaluated the proliferation of UCMSCs with Cellhesion<sup>®</sup> MS, microcarriers, and U-bottom plates. The cell growth of UCMSCs using microcarriers was significantly better than with Cellhesion<sup>®</sup> MS and U-bottom plates at four and seven days ( $p < 0.001$ ) (Figure 5B). From the viewpoint of spheroid culture, the cell growth of UCMSCs with Cellhesion<sup>®</sup> MS was significantly better than with U-bottom plates at seven days ( $p < 0.01$ ) (Figure 5B). Next, to verify the characteristics of UCMSCs on Cellhesion<sup>®</sup> MS in a culture bag, we evaluated the expression of stemness-related genes (OCT4 and NANOG) and of CXCR4. The expression levels of OCT4, NANOG, and CXCR4 in UCMSCs with Cellhesion<sup>®</sup> MS were significantly upregulated, compared with microcarrier and U-bottom plate culture ( $p < 0.05$ ,  $p < 0.01$  or  $p < 0.001$ , respectively) (Figure 5C). The secretion levels of PGE<sub>2</sub> from UCMSCs with Cellhesion<sup>®</sup> MS were significantly higher

than in microcarrier and U-bottom plate culture, whether with  $TNF\alpha$  ( $p < 0.001$  and  $p < 0.05$ , respectively) or without  $TNF\alpha$  ( $p < 0.01$  and  $p < 0.05$ , respectively) (Figure 5D). The amount of bFGF secreted from UCMSCs with Cellhesion<sup>®</sup> MS was significantly higher than with microcarrier and U-bottom plate culture ( $p < 0.001$ ) (Figure 5D). Lastly, we investigated the effects of changes of medium volume on cell growth using Cellhesion<sup>®</sup> MS. It was found that the UCMSC growth rate was the same, whether changing half the medium volume or carrying out full medium replacement (Figure 5E). These results suggest that an MSC culture using Cellhesion<sup>®</sup> MS is a viable new culture system. This would facilitate large-scale culture of UCMSCs that gain stemness- and migration-related genes and secrete far more paracrine factors.

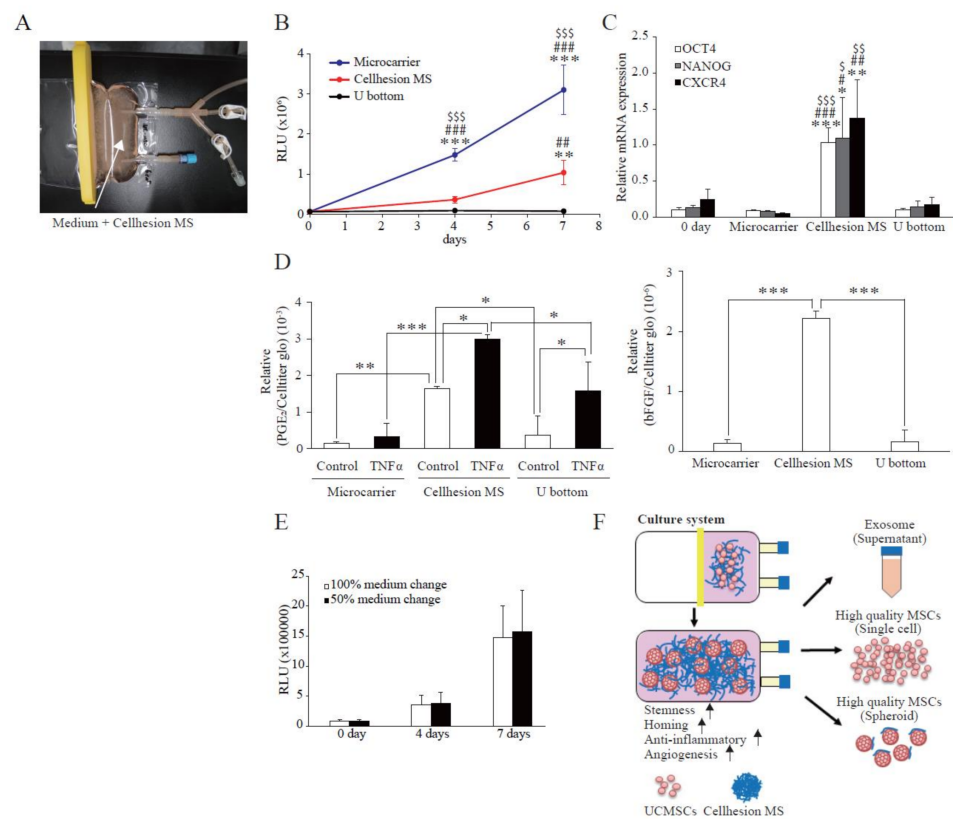


**Figure 5.** Scaled-up culture of UCMSCs using a culture bag to produce a closed culture system. (A) An image of the culture bag configuration. White arrows indicate medium containing 0.05% Cellhesion<sup>®</sup> MS. (B) Comparison of cell growth in each culture method. The number of UCMSCs was measured using an ATP assay. \*\*  $p < 0.01$ , \*\*\*  $p < 0.001$ , compared with day zero. ###  $p < 0.01$ , ###  $p < 0.001$ , compared with U-bottom plate. \$\$\$  $p < 0.001$ , compared with Cellhesion<sup>®</sup> MS. (C) The expression levels of NANOG, OCT4, and CXCR4 in UCMSCs on Cellhesion<sup>®</sup> MS increased, compared with microcarrier and U-bottom plate culture. The expression levels of NANOG, OCT4, and CXCR4 mRNA in UCMSCs were determined by real-time RT-PCR and normalized to GAPDH mRNA levels. \*  $p < 0.05$ , \*\*  $p < 0.01$ , \*\*\*  $p < 0.001$ , compared with day zero. #  $p < 0.05$ , ##  $p < 0.01$ , ###  $p < 0.001$ , compared with microcarrier. \$  $p < 0.05$ , \$\$  $p < 0.01$ , \$\$\$  $p < 0.001$ , compared with U-bottom plate. (D) The secretion levels of PGE<sub>2</sub> and bFGF from UCMSCs with Cellhesion<sup>®</sup> MS increased, compared with microcarrier and U-bottom plate culture. The secretion levels of PGE<sub>2</sub> and bFGF from UCMSCs were measured by ELISA and normalized with an ATP assay. \*  $p < 0.05$ , \*\*  $p < 0.01$ , \*\*\*  $p < 0.001$ , compared with control or  $TNF\alpha$  in microcarrier or U-bottom plate culture. (E) The number of UCMSCs was the same, for 50% and 100% volume medium replacement during the culture period. The number of UCMSCs was measured using an ATP assay in both conditions. (F) Schematic of a closed culture system using Cellhesion<sup>®</sup> MS. Data show mean averages  $\pm$  SD for three independent experiments.

#### 4. Discussion

Chitin is a long-chain polymer of N-acetylglucosamine, a derivative of glucose and a biodegradable bioadhesive and biocompatible material [17]. It has been approved by the U.S. Food and Drug Administration (FDA) for human use [18]. There are several reports about MSCs and chitin-based materials. One example is a deacetylated derivative of chitin: chitosan. Some researchers have reported that ADMSCs and placenta derived MSCs formed spheroids on chitosan, which is coated with hyaluronan, and that this material maintained OCT4, SOX2, and NANOG expression levels [19]. Other research demonstrated that the expression levels of CXCR4 were upregulated on a chitosan membrane [20]. In line with these reports, we investigated the effects of Cellhesion<sup>®</sup> MS. UCMSCs formed spheres on Cellhesion<sup>®</sup> MS and increased the expression of OCT4, NANOG, and CXCR4. In addition to the above reports, it has been reported that OCT4 and SOX2-overexpressing ADMSCs have a higher anti-inflammatory effect than control ADMSCs [21]. From this report it follows that the higher expression levels of OCT4 observed in UCMSCs with Cellhesion<sup>®</sup> MS could affect the anti-inflammatory effect.

One benefit of using Cellhesion<sup>®</sup> MS in MSCs 3D culture is affecting the features and quality of MSCs by enhancing cell–cell interactions. Traditional 3D-spheroid culture methods, such as the hanging drop and low attachment plate, can change MSC features such as stemness gene expression and secretion of paracrine factors [22]. In this study we observed spheres of UCMSCs on Cellhesion<sup>®</sup> MS, similar to traditional spheroid culture methods. In accordance with previous reports, a Cellhesion<sup>®</sup> MS-mediated 3D culture increases OCT4 and NANOG expression levels (Figures 1D, 4C and 5C) and paracrine factors (Figures 2A,B, 4D and 5D). In addition, unlike conventional 3D spheroid methods, Cellhesion<sup>®</sup> MS culture enables UCMSCs not only to increase stemness-related genes and to secrete far more paracrine factors, but also to grow, as opposed to U-bottom plate culture (Figure 5B–D). The possible mechanism of this promotion may be due to the change of cellular morphology. There is report showed that MSCs in spheroids are more secretory than their monolayer counterparts [23]. The types of MSC 3D cultures that is biomaterials, also produce similar effects. The MSC in the middle of the spheroids and in the biomaterials, both experience limited adhesion and spreading, lack of polarization, less cellular strain due to less mechanical stiffness of the surroundings, a gradient of paracrine factors, and ultimately a common increase in mediators PGE<sub>2</sub>, hepatocyte growth factors. MSCs in spheroids had different mechanotransduction than the monolayer counterparts, which may regulate the interrelated signaling pathways, including RhoA/ROCK, Akt/Erk, or YAP/TAZ to affect the paracrine effect of MSCs [24]. We will investigate the detailed mechanism in further studies.

Another benefit of applying Cellhesion<sup>®</sup> MS to large-scale high quality MSC culture is cost reduction. Some researchers have reported that it's important to manufacture high-quality MSCs in massive volume and at lower costs to increase frequency of use [25]. For large-scale UCMSCs culture conditions, the cost of production space and labor account for large proportion. Cellhesion<sup>®</sup> MS 3D cell culture method provides the possibility to expand UCMSCs in bioreactor tank, which could save space and reduce manual operation compared to 2D monolayer culture system, thus, 3D cell culture could save a lot of costs.

PGE<sub>2</sub> is a bioactive lipid produced from arachidonic acid, with cyclooxygenase (COX) as the rate-limiting enzyme. PGE<sub>2</sub> is an immunosuppressive factor secreted by MSCs. By reducing the activation and proliferation of NK and T cells, it is possible to realize not only GVHD treatment but also allogeneic transplantation [10,26]. UCMSCs exhibit a higher expression of the OCT4 gene than BMMSCs, but also have a greater ability to suppress the proliferation of T cells involved in inflammation [10]. PGE<sub>2</sub> is an essential factor in the suppression of T cell proliferation related to inflammation, suggesting that it is better to use UCMSCs for allogeneic transplantation than BMMSCs [10]. Furthermore, it has been reported that PGE<sub>2</sub> plays a prominent role in the mechanism of various immunomodulatory factors [10] and has an important role in therapy for various diseases. It has been reported that MSCs administered to GVHD model mice show therapeutic effects, with PGE<sub>2</sub> being

one of the main therapeutic mediators [27]. In addition, it has been reported that PGE<sub>2</sub> is a marker for predicting therapeutic effects in the treatment of traumatic brain injury with MSCs [28]. PGE<sub>2</sub> is also known to promote the migration of MSCs via FAK and ERK1/2 [29] and may increase the efficiency of its own migration. The combination of UCMSCs and 3D culture using Cellhesion<sup>®</sup> MS is the most suitable method of producing allogeneic MSCs, because of their ability to secrete high levels of PGE<sub>2</sub>. TSG-6 is a representative secretory factor that exhibits immunosuppressive activity and has been reported to be a factor in the therapeutic effect of MSCs on various diseases [30]. It has been reported that when human BMMSCs are administered to acute pancreatitis model mice, TSG-6 acts as a major secretory factor and exhibits a therapeutic effect [31]. In addition, it has been reported that human BMMSCs produce a therapeutic effect via TSG-6 in lipopolysaccharide-induced lung injury model mice [32]. The amount of PGE<sub>2</sub>, TSG-6, bFGF and Angiogenin secreted from MSCs cultured with Cellhesion<sup>®</sup> MS is higher than in MSCs in monolayer culture, indicating that a Cellhesion<sup>®</sup> MS culture is more efficient in producing cells to treat diseases such as ischemic heart disease and cartilage injury [33,34]. Besides that, the 3D culture methods also tries to reduce the gap between in vitro and in vivo drug testing models.

Large-scale MSC culture has been used to produce not only MSCs but also EVs (from culture supernatants) as therapeutics [7,8]. The medium used for culturing MSCs typically contains bFGF [35]. bFGF is an important factor for promoting MSC proliferation and the maintenance of stemness [36]. However, it is expensive and must be continually added to the culture medium because of its rapid degradation [37]. Therefore, the cost of bFGF is an important component of the total cost of MSC production. Recently, low molecular weight compounds that exhibit bFGF-like effects have been screened [38]. In the culture system using Cellhesion<sup>®</sup> MS, MSCs secrete bFGF at a practical level; it is likely that the amount of medium exchange can be considerably reduced with Cellhesion<sup>®</sup> MS. Cell growths with 50% volume media changes and with 100% medium changes gave the same results (Figure 5E). This has great merit in terms of reducing the cost of medium in MSC production, compared with monolayer culture and other culture methods. Thus, our culture method can also be applied to EV production, which enables a scaled-up culture and reduced culture costs.

Limitation still existed in this study, for example, there was sample difference. In this study, we used commercial UCMSCs to establish the Cellhesion<sup>®</sup> MS culture system. Then, UCMSCs from donors were used to verify this 3D culture system, because UC-MSCs from donors will be used in the clinical cell therapy and there will be individual difference. Our experiment results (Section 3.4) showed that UCMSCs from donors could be cultured and expanded on Cellhesion<sup>®</sup> MS. Compared to 2D monolayer culture, UCMSCs culture on Cellhesion<sup>®</sup> MS had higher NANOG, OCT4 gene expression and PGE<sub>2</sub>, bFGF secretion. This demonstrated the 3D culture system based on Cellhesion<sup>®</sup> MS has general applicability. The results also demonstrated that it is necessary to screen UCMSCs with higher viability to achieve better clinical effect. In the future, we will test more samples from donors to establish a UCMSCs screening criteria according to big data of quality study, which will provide UCMSCs seeds for scale-up cultivation in consistent quality. Besides that, we will construct a closed culture system for UCMSCs using Cellhesion<sup>®</sup> MS (Figure 5F). The open style of monolayer culture methods complicates the production of cells, which increases the cost of quality testing and limits the production equipment to prevent cross-contamination. Our study suggests that high-quality UCMSCs can be cultured by combining oxygen-permeable bags and Cellhesion<sup>®</sup> MS in a closed system culture model.

## 5. Conclusions

The 3D culture method using Cellhesion<sup>®</sup> MS enables UCMSCs to secrete high levels of immunosuppressive factors, suggesting the possibility of producing MSCs with superior allogeneic properties. In addition, cells grown using this culture method were able to gain stemness expression, unlike other culture methods, and to produce the high levels of bFGF

secretion necessary for MSC proliferation. It is expected that this culture method may become an important technology in the development of a closed culture system.

**Author Contributions:** Conceived and designed the experiments: K.K., T.K., S.G., D.H. Performed the experiments: K.K., T.K., S.G., D.H., M.I., S.L. Analyzed the data: K.K., T.K., S.G., D.H., M.I. Prepared the paper: K.K., T.K., S.G., D.H., M.I., M.H., M.O., D.C. All authors have read and agreed to the published version of the manuscript.

**Funding:** This work was supported by the Nissan Chemical Corporation and BOE Regenerative Medicine Technology Co., Ltd.

**Institutional Review Board Statement:** The use of the human umbilical cord samples was approved by the Ethics Committees of the Oasis International Hospital (File number: LLPJ2018[001]).

**Informed Consent Statement:** Informed consent was obtained from all subjects involved in the study.

**Data Availability Statement:** The data that support the findings of this study are available from the corresponding authors, Tatsuro Kanaki, and Dehua Chang, upon reasonable request.

**Acknowledgments:** The authors thank M. Matsumoto for technical assistance.

**Conflicts of Interest:** The authors declare no conflict of interest.

## References

1. Prockop, D.J. Marrow stromal cells as stem cells for nonhematopoietic tissues. *Science* **1997**, *276*, 71–74. [[CrossRef](#)] [[PubMed](#)]
2. Campagnoli, C.; Roberts, I.A.; Kumar, S.; Bennett, P.R.; Bellantuono, I.; Fisk, N.M. Identification of mesenchymal stem/progenitor cells in human first-trimester fetal blood, liver, and bone marrow. *Blood* **2001**, *98*, 2396–2402. [[CrossRef](#)] [[PubMed](#)]
3. Zuk, P.A.; Zhu, M.; Ashjian, P.; Ugarte, D.A.; Huang, J.I.; Mizuno, H.; Alfonso, Z.C.; Fraser, J.K.; Benhaim, P.; Hedrick, M.H. Human adipose tissue is a source of multipotent stem cells. *Mol. Biol. Cell.* **2002**, *13*, 4279–4295. [[CrossRef](#)] [[PubMed](#)]
4. Olmar, R.E.I.; Beroud, J.; Stoltz, J.-F.; Menu, P.; Velot, E.; Decot, V. Umbilical cord mesenchymal stem cells: The new gold standard for mesenchymal stem cell-based therapies? *Tissue Eng. Part B Rev.* **2014**, *20*, 523–544.
5. Kanelidis, A.J.; Premer, C.; Lopez, J.; Balkan, W.; Hare, J.M. Route of Delivery Modulates the Efficacy of Mesenchymal Stem Cell Therapy for Myocardial Infarction: A Meta-Analysis of Preclinical Studies and Clinical Trials. *Circ. Res.* **2017**, *120*, 1139–1150. [[CrossRef](#)]
6. Wang, L.; Ting, C.H.; Yen, M.E.; Liu, K.O.; Sytwu, H.U.; Wu, K.K.; Yen, B.L. Human mesenchymal stem cells (MSCs) for treatment towards immune- and inflammation-mediated diseases: Review of current clinical trials. *J. Biomed. Sci.* **2016**, *23*, 76. [[CrossRef](#)]
7. Lai, R.C.; Arslan, F.; Lee, M.M.; Sze, N.S.K.; Choo, A.; Chen, T.S.; Salto-Tellez, M.; Timmers, L.; Lee, C.N.; El Oakley, R.M.; et al. Exosome secreted by MSC reduces myocardial ischemia/reperfusion injury. *Stem. Cell Res.* **2010**, *4*, 214–222. [[CrossRef](#)]
8. Katsuda, T.; Kosaka, N.; Takeshita, F.; Ochiya, T. The therapeutic potential of mesenchymal stem cell-derived extracellular vesicles. *Proteomics* **2013**, *13*, 1637–1653. [[CrossRef](#)]
9. Zhang, J.; Huang, X.; Wang, H.; Liu, X.; Zhang, T.; Wang, Y.; Hu, D. The challenges and promises of allogeneic mesenchymal stem cells for use as a cell-based therapy. *Stem. Cell. Res. Ther.* **2015**, *6*, 234. [[CrossRef](#)]
10. Chen, K.; Wang, D.; Du, W.T.; Han, Z.-B.; Ren, H.; Chi, Y.; Yang, S.G.; Zhu, D.; Bayard, F.; Han, Z.C. Human umbilical cord mesenchymal stem cells hUC-MSCs exert immunosuppressive activities through a PGE2-dependent mechanism. *Clin. Immunol.* **2010**, *135*, 448–458. [[CrossRef](#)]
11. Zhou, Y.; Chan, H.; Li, H.; Wu, Y. 3D culture increases pluripotent gene expression mesenchymal stem cells through relaxation of cytoskeleton tension. *J. Cell. Mol. Med.* **2017**, *21*, 1073–1084. [[CrossRef](#)]
12. Sethe, S.; Scutt, A.; Stolzing, A. Aging of mesenchymal stem cells. *Ageing Res. Rev.* **2006**, *5*, 91–116. [[CrossRef](#)] [[PubMed](#)]
13. Ksiazek, K. A comprehensive review on mesenchymal stem cell growth and senescence. *Rejuvenation Res.* **2009**, *12*, 105–116. [[CrossRef](#)] [[PubMed](#)]
14. Feng, J.; Yang, S.; Xu, L.; Tian, H.; Sun, L.; Tang, X. Role of caspase-3 inhibitor in induced anoikis of mesenchymal stem cells in vitro. *J. Huazhong Univ. Sci. Technol. Med. Sci.* **2007**, *27*, 183–185. [[CrossRef](#)] [[PubMed](#)]
15. Kim, E.S.; Kida, K.; Mok, J.; Seong, Y.; Jo, S.Y.; Kanaki, T.; Horikawa, M.; Kim, K.-H.; Kim, T.M.; Park, T.S.; et al. Cellhesion VP enhances the immunomodulating potential of human mesenchymal stem cell-derived extracellular vesicles. *Biomaterials* **2021**, *271*, 120742. [[CrossRef](#)] [[PubMed](#)]
16. Bartosh, T.J.; Ylöstalo, J.H.; Mohammadipoor, A.; Bazhanov, N.; Coble, K.; Claypool, K.; Lee, R.H.; Choi, H.; Prockop, D.J. Aggregation of human mesenchymal stromal cells (MSCs) into 3D spheroids enhances their antiinflammatory properties. *Proc. Natl. Acad. Sci. USA* **2010**, *107*, 13724–13729. [[CrossRef](#)] [[PubMed](#)]
17. Jayakumar, R.; Chennazhi, K.P.; Srinivasan, S.; Nair, S.V.; Furuike, T.; Tamura, H. Chitin scaffolds in tissue engineering. *Int. J. Mol. Sci.* **2011**, *12*, 1876–1887. [[CrossRef](#)]

18. Shao, H.U.; Lee, Y.U.; Chen, C.H.; Wang, J.Y.; Young, T.A. Modulation of gene expression and collagen production of anterior cruciate ligament cells through cell shape changes on polycaprolactone/chitosan blends. *Biomaterials* **2010**, *31*, 4695–4705. [[CrossRef](#)]
19. Huang, G.U.; Dai, L.I.; Yen, B.L.; Hsu, S.H. Spheroid formation of mesenchymal stem cells on chitosan and chitosan-hyaluronan membranes. *Biomaterials* **2011**, *32*, 6929–6945. [[CrossRef](#)]
20. Yeh, H.S.; Liu, B.I.; Sieber, M.; Hsu, S.H. Substrate-dependent gene regulation of self-assembled human MSC spheroids on chitosan membranes. *BMC Genom.* **2014**, *15*, 10. [[CrossRef](#)]
21. Li, Q.; Han, S.E.; Song, W.O.; Park, S.A.; Ryu, M.I.; Youn, H.W. Anti-inflammatory Effects of Oct4/Sox2-overexpressing Human Adipose Tissue-derived Mesenchymal Stem Cells. *In Vivo* **2017**, *31*, 349–356. [[CrossRef](#)] [[PubMed](#)]
22. Petrenko, Y.; Syková, E.; Kubinová, Š. The therapeutic potential of three-dimensional multipotent mesenchymal stromal cell spheroids. *Stem. Cell. Res. Ther.* **2017**, *8*, 94. [[CrossRef](#)] [[PubMed](#)]
23. Madrigal, M.; Rao, K.S.; Riordan, N.H. A review of therapeutic effects of mesenchymal stem cell secretions and induction of secretory modification by different culture methods. *J. Transl. Med.* **2014**, *12*, 260. [[CrossRef](#)] [[PubMed](#)]
24. Saidova, A.A.; Vorobjev, I.A. Lineage Commitment, Signaling Pathways, and the Cytoskeleton Systems in Mesenchymal Stem Cells. *Tissue Eng. Part B Rev.* **2020**, *26*, 13–25. [[CrossRef](#)] [[PubMed](#)]
25. Olsen, T.R.; Ng, K.S.; Lock, L.T.; Ahsan, T.; Rowley, J.A. Peak MSC-Are We There Yet? *Front. Med.* **2018**, *5*, 178. [[CrossRef](#)] [[PubMed](#)]
26. Spaggian, G.M.; Capobianco, A.; Abdelrazik, H.; Becchetti, F.; Mingari, M.C.; Moretta, L. Mesenchymal stem cells inhibit natural killer-cell proliferation, cytotoxicity, and cytokine production: Role of indoleamine 2,3-dioxygenase and prostaglandin E2. *Blood* **2008**, *111*, 1327–1333. [[CrossRef](#)]
27. Auletta, J.J.; Eid, S.K.; Wuttisarnwattana, P.; Silva, I.; Metheny, L.; Keller, M.D.; Guardia-Wolff, R.; Liu, C.; Wang, F.; Bowen, T.; et al. Human Mesenchymal Stromal Cells Attenuate Graft-Versus-Host Disease and Maintain Graft-Versus-Leukemia Activity Following Experimental Allogeneic Bone Marrow Transplantation. *Stem. Cells* **2015**, *33*, 601–614. [[CrossRef](#)]
28. Kota, D.J.; Prabhakara, K.S.; Toledano-Furman, N.; Bhattarai, D.; Chen, Q.; DiCarlo, B.; Smith, P.; Triolo, F.; Wenzel, P.L.; Cox, C.S., Jr.; et al. Prostaglandin E2 Indicates Therapeutic Efficacy of Mesenchymal Stem Cells in Experimental Traumatic Brain Injury. *Stem. Cells* **2017**, *35*, 1416–1430. [[CrossRef](#)]
29. Lu, X.; Han, J.; Xu, X.; Xu, J.; Liu, L.; Huang, Y.; Yang, Y.; Qiu, H. PGE2 Promotes the Migration of Mesenchymal Stem Cells through the Activation of FAK and ERK1/2 Pathway. *Stem. Cells Int.* **2017**, *2017*, 8178643. [[CrossRef](#)]
30. Song, W.J.; Li, Q.; Ryu, M.O.; Ahn, J.O.; Ha Bhang, D.; Chan Jung, Y.; Youn, H.Y. TSG-6 Secreted by Human Adipose Tissue-derived Mesenchymal Stem Cells Ameliorates DSS-induced colitis by Inducing M2 Macrophage Polarization in Mice. *Sci. Rep.* **2017**, *7*, 5187. [[CrossRef](#)]
31. He, Z.; Hua, J.; Qian, D.; Gong, J.; Lin, S.; Xu, C.; Wei, G.; Meng, H.; Yang, T.; Zhou, B.; et al. Intravenous hMSCs Ameliorate Acute Pancreatitis in Mice via Secretion of Tumor Necrosis Factor- $\alpha$  Stimulated Gene/Protein 6. *Sci. Rep.* **2016**, *6*, 38438. [[CrossRef](#)] [[PubMed](#)]
32. Lee, R.H.; Pulin, A.A.; Seo, M.J.; Kota, D.J.; Ylostalo, J.; Larson, B.L.; Semprun-Prieto, L.; Delafontaine, P.; Prockop, D.J. Intravenous hMSCs improve myocardial infarction in mice because cells embolized in lung are activated to secrete the anti-inflammatory protein TSG-6. *Cell. Stem. Cell.* **2009**, *5*, 54–63. [[CrossRef](#)] [[PubMed](#)]
33. Guo, Y.; Yu, Y.; Hu, S.; Chen, Y.; Shen, Z. The therapeutic potential of mesenchymal stem cells for cardiovascular diseases. *Cell. Death Dis.* **2020**, *11*, 349. [[CrossRef](#)] [[PubMed](#)]
34. Zhang, R.; Ma, J.; Han, J.; Zhang, W.; Ma, J. Mesenchymal stem cell related therapies for cartilage lesions and osteoarthritis. *Am. J. Transl. Res.* **2019**, *11*, 6275–6289. [[PubMed](#)]
35. Nekanti, U.; Mohanty, L.; Venugopal, P.; Balasubramanian, S.; Totey, S.; Ta, M. Optimization and scale-up of Wharton's jelly-derived mesenchymal stem cells for clinical applications. *Stem. Cell Res.* **2010**, *5*, 244–254. [[CrossRef](#)] [[PubMed](#)]
36. Tasso, R.; Gaetani, M.; Molino, E.; Cattaneo, A.; Monticone, M.; Bachi, A.; Cancedda, R. The role of bFGF on the ability of MSC to activate endogenous regenerative mechanisms in an ectopic bone formation model. *Biomaterials* **2012**, *33*, 2086–2096. [[CrossRef](#)]
37. Xu, H.E.; Chen, P.I.; ZhuGe, D.E.; Zhu, Q.U.; Jin, B.I.; Shen, B.I.; Xiao, J.; Zhao, Y.I. Liposomes with Silk Fibroin Hydrogel Core to Stabilize bFGF and Promote the Wound Healing of Mice with Deep Second-Degree Scald. *Adv. Healthc. Mater.* **2017**, *6*, 1700344. [[CrossRef](#)]
38. Imagama, S.; Ogino, R.; Ueno, S.; Murayama, N.; Takemoto, N.; Shimmyo, Y.; Kadoshima, T.; Tamura, S.; Kuroda, M.; Matsuyama, Y.; et al. Systemic treatment with a novel basic fibroblast growth factor mimic small-molecule compound boosts functional recovery after spinal cord injury. *PLoS ONE* **2020**, *15*, e0236050. [[CrossRef](#)]